European Journal of Medicinal Chemistry 65 (2013) 119–133

Contents lists available at SciVerse ScienceDirect

European Journal of Medicinal Chemistry

journal homepage: http://www.elsevier.com/locate/ejmech

Original article

2,5,6-Trisubstituted imidazo[2,1-*b*][1,3,4]thiadiazoles: Search for antihyperlipidemic agents

Harun M. Patel [a], Malleshappa N. Noolvi [b,*], Anjali Goyal [c], B.S. Thippeswamy [d]

[a] *Division of Computer Aided Drug Design, Department of Pharmaceutical Chemistry, R.C. Patel Institute of Pharmaceutical Education and Research, Shirpur, Dhule 425405, Maharashtra, India*
[b] *Department of Pharmaceutical Chemistry, Shree Dhanvantary Pharmacy College, Kim, Surat 3941110, Gujarat, India*
[c] *Department of Pharmaceutical Chemistry, ASBASJSM College of Pharmacy, Bela, Ropar 140111, Punjab, India*
[d] *Department of Pharmacology, Sree Siddagang College of Pharmacy, Tumkur 572102, Karnataka, India*

ARTICLE INFO

Article history:
Received 11 October 2012
Received in revised form
4 April 2013
Accepted 8 April 2013
Available online 18 April 2013

Keywords:
Synthesis imidazo[2,1-*b*][1,3,4]thiadiazole
Hyperlipedimia
QSAR
Atherogenic index

ABSTRACT

A novel series of 2,5,6-trisubstituted imidazo[2,1-*b*][1,3,4]thiadiazoles **4**(**a**–**d**) and **7**(**a**–**i**) were rationally designed through QSAR based pharmacophore approach and synthesized from 5-(1,3-benzodioxol-5-yl)-[1,3,4]thiadiazol-2-amine (**1**). The structures of these compounds were established by IR, ^{1}H NMR, ^{13}C NMR, HRMS technique. All the compounds were evaluated for their in vitro antihyperlipidemic activity using trition induced hyperlipidemic model. The newly synthesized title compound **7d**, **7e** and **7h** showed a significant decrease in the serum, TCH, TG LDL and VLDL values along with an increase in serum HDL levels as compared to standard drug Fenofibrate. The treated groups also showed significant decrease in the atherogenic index, LDL:HDL risk ratios and the level of SGOT, SGPT and ALP activities compared to cholesterol induced hyperlipidemic control group.

1. Introduction

Hyperlipidemia is a major cause of atherosclerosis and atherosclerosis-associated conditions such as coronary heart disease, ischemic cerebrovascular disease, and peripheral vascular disease [1]. A causal relationship between the elevated plasma lipids and the development of atherosclerotic plaques has been well established. Hyperlipidemia is an elevation of lipids in the bloodstream and these lipids include fats, fatty acids, cholesterol, cholesterol esters, phospholipids, and triglycerides [2,3]. Therefore, agents that increase HDL cholesterol concentration in the blood and thereby ratio of HDL cholesterol to total cholesterol (H/C) would have promising therapeutic utility as antihyperlipidemic agents [4,5]. Despite significant medical advances, heart attacks due to coronary artery disease (due to atherosclerosis that affects the arteries supplying blood to the heart) and stroke (due to atherosclerosis that affects the arteries supplying blood to the brain) are responsible for more deaths than all other causes combined. In addition to this; different cholesterol lowering drugs or non-pharmacological treatments can significantly reduce morbidity from CHD, thus providing a causal role for cholesterol in coronary events. During recent years, there have been intense investigations on thiadiazole and imidazo[2,1-*b*][1,3,4]thiadiazole compounds carried out, many of which are known to possess interesting biological properties such as antimicrobial [6,7], antitubercular [8,9], anti-inflammatory [10,11], anticonvulsant [12,13], antihypertensive [14,15], and anticancer activities [16].

In view of the above facts and in continuation of our research for various biologically active molecules [9,17–19] and encouraging QSAR and docking study reported in the literature by Kathia M. Honorio et al. [20,21] has prompted us to synthesize novel molecules of fused imidazo[2,1-*b*][1,3,4]thiadiazole and screen for their in vitro antihyperlipidemic activity (Fig. 1).

2. Rationale and designing

The Farnesoid-X-Receptor (FXR) is an attractive drug target for the development of novel therapeutic agents for the treatment of dyslipidemia and cholestasis. Hologram Quantitative Structure Activity Relationship (HQSAR) studies were conducted on a series of potent FXR activators originated from natural product-like libraries by Kathia M. Honorio et al. [21]. In HQSAR, it is possible to visualize the individual contribution to activity of each atom in a

* Corresponding author. Tel.: +91 8141175355; fax: +91 1881263655.
E-mail addresses: mnoolvi@yahoo.co.uk, mallesh7301@rediffmail.com (M.N. Noolvi).

0223-5234/$ – see front matter © 2013 Elsevier Masson SAS. All rights reserved.
http://dx.doi.org/10.1016/j.ejmech.2013.04.020

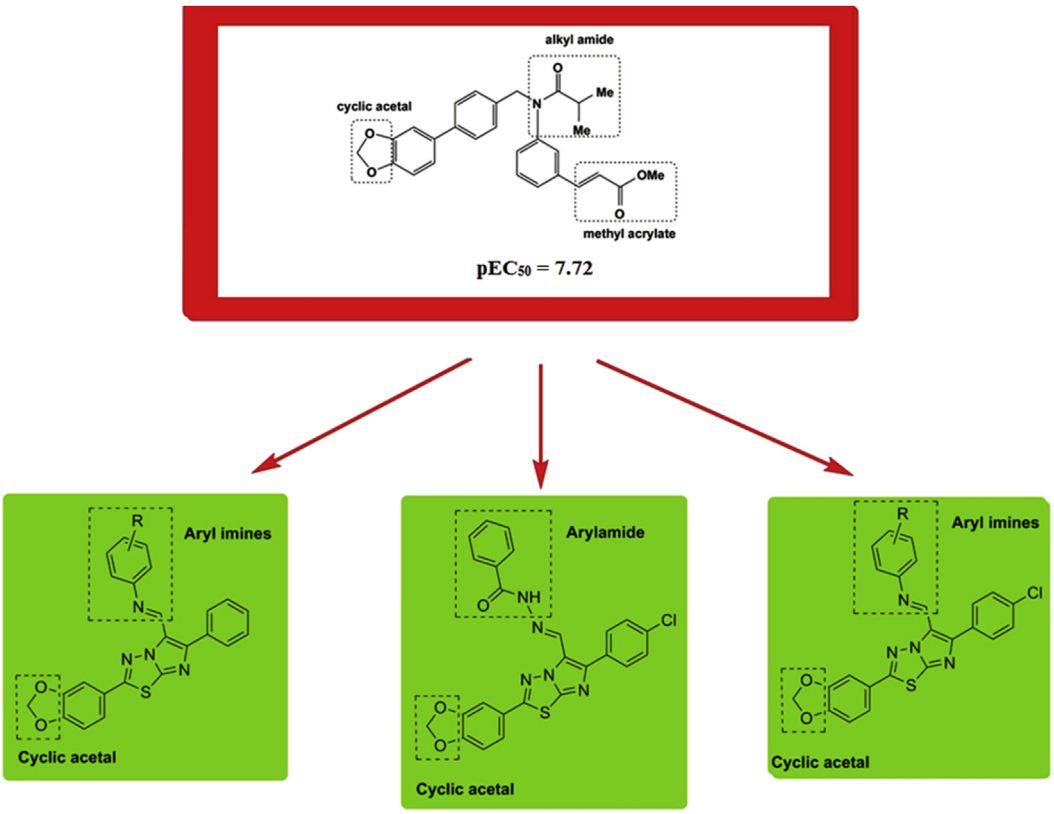

Fig. 1. Synthesized fused imidazo[2,1-*b*][1,3,4]thiadiazoles based upon QSAR model proposed by Kathia M. Honorio et al. [21].

given molecule of the data set through the generation of contribution maps. They suggested that one fragment of the molecular structure, represented by the 1,3-benzodioxol moiety, is strongly related to the biological activity having $pEC_{50} = 7.72$ as shown in Fig. 1. An important role of a QSAR model, besides predicting the activities of untested molecules, is to provide hints about what molecular fragments are directly related to biological activity. This information, combined with knowledge of synthetic chemistry, promoted us to the synthesis new 2,5,6-trisubstituted imidazo[2,1-*b*][1,3,4]thiadiazoles containing 1,3-benzodioxol moiety as novel FXR ligands having improved potency.

3. Chemistry

Synthesis of fused imidazo[2,1-*b*][1,3,4]thiadiazole **4**(**a**–**d**) and **7**(**a**–**i**) is outlined in Scheme 1. 5-(Benzo[*d*][1,3]dioxol-5-yl)-[1,3,4]thiadiazol-2-amine **1** is prepared as per the reported method [22]. Condensation of **1** with respective bromoacetyl compound in ethanol and dimethylformamide yields imidazo thiadiazole **2** and **5** in good yields [23]. Vilsmeier–Hack reaction of imidazo thiadiazole **2** and **5**, in DMF and $POCl_3$ provided respective 5-formyl derivatives **3** and **6** [23]. The aldehyde functional group when treated with amines gave the corresponding imine derivatives **4**(**a**–**d**) and **7**(**a**–**i**). The detail reaction mechanism is depicted in physical data is given in Table 1.

4. Pharmacology

4.1. Experimental animals

Wistar albino adult male rats weighing 200–250 g were obtained from the animal house department of pharmacology, Sree Siddagang College of Pharmacy, Tumkur (Karnataka) India. The animal were grouped and housed in polyacrylic cages (38 × 23 × 10 cm) with not more than six animals per cage and maintained under standard laboratory conditions (temperature 25 ± 2 °C) with dark and light cycle (14/10 h). They were allowed free access to standard dry pellet diet and water ad libitum. The mice were acclimatized to laboratory condition for 10 days before commencement of experiment. The experimental protocol was approved by Institutional Animal Ethical Committee (IAEC No. SSCP/IAEC/2010-11/52) constituted under CPCSEA.

4.2. Induction of hyperlipidemia

Hyperlipidemia was induced in Wistar albino rats by single intraperitoneal injection of freshly prepared solution of Triton-X-100 (100 mg/kg) in physiological saline solution after overnight fasting for 18 h. The animals were divided into four groups of six rats each. The first group was given standard pellet diet, water and orally administered with 5% CMC. The second group was given a single dose of triton administered at a dose of 100 mg/kg, i.p. After 72 h of triton injection, this group received a daily dose of 5% CMC (p.o.) for 7 days. The third group was administered a daily dose of synthesized compounds 250 mg/kg suspended in 5% CMC (p.o.) for 7 days, after inducing hyperlipidemia. Fourth group was administered with the standard Fenofibrate 250 mg/kg (p.o.) for 7 days [24].

4.3. Collection of blood

At the end of experimental period, blood was collected by retro orbital sinus puncture, under mild ether anesthesia. The serum was separated by centrifugation at 2500× *g* for 15 min at 4 °C. Then serum samples were collected and assayed for total cholesterol,

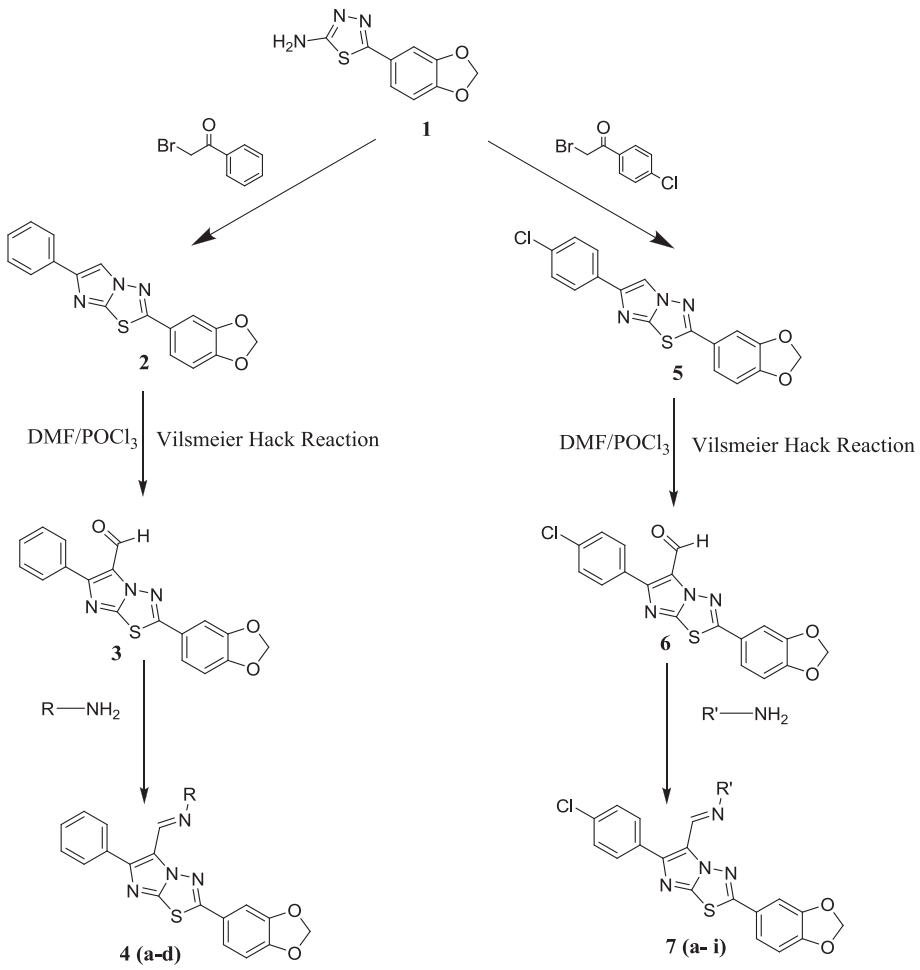

4a: R = -C_6H_5
4b: R = -C_6H_5-4-Br
4c: R = -C_6H_5-4-OCH_3
4d: R= -C_6H_5-4-CH_3

7a: R' = -C_6H_5-4-CH_3
7b: R' = -C_6H_5-3-OCH_3
7c: R' = -C_6H_5-3-CH_3
7d: R'= -C_6H_5-4-SO_2NH_2
7e: R' = -C_6H_5-4-COOH
7f: R' = -NHCO-C_6H_5
7g: R' = -C_6H_5-4-NO_2
7h: R' = -C_6H_5-3-Cl-4-F
7i: R' = -C_6H_5-4-Br

Scheme 1. General synthetic route for the synthesis of the compounds **4**(**a**–**d**) and **7**(**a**–**i**).

triglycerides, phospholipids, high-density lipoprotein (HDL), low-density lipoprotein (LDL), very low-density lipoprotein (VLDL) using standard protocol methods used for various biochemical experiments. The animals were then sacrificed and the liver collected [25].

4.4. Histopathological observation of liver

Animals were euthanized under ether anesthesia and the liver was dissected out immediately. For histopathological analysis, the liver tissues were fixed in 10% formalin at room temperature. The tissue was embedded in paraffin, sectioned by 3–4 μm thickness, and mounted on the glass microscope slides using standard histological techniques [26]. The sections were stained with hematoxylin-eosin and examined using light microscopy at 200× magnitude. These light-microscopic fields were assessed by an image analyzer (Pro® Plus Version 4.5. Media Cybernetics, MD, USA) on each section.

4.5. Biochemical analysis

The serum was assayed for total cholesterol, triglycerides, high-density lipoprotein (HDL), low-density lipoprotein (LDL), very low-density lipoprotein (VLDL) as per the reported method [27–29]. Hepatotoxicity was evaluated by measuring alanine transferase [30], aspartate transferase [31] and alkaline phosphatase [32] levels in serum.

5. Docking study

The molecular docking tool, GLIDE (Schordinger Inc., USA) (2009) was used for ligand docking studies into the FXR binding pocket. The crystal structures of FXR were obtained from protein

Table 1
Physical data of synthesized compounds **4**(**a**–**d**) and **7**(**a**–**i**).

Sr. No.	Compound	Molecular formula	Molecular weight	Melting point (°C)	Yield (%)
4a	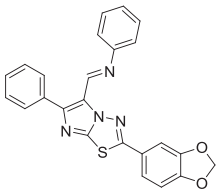	$C_{24}H_{16}N_4O_2S$	424.4744	123–125	67
4b	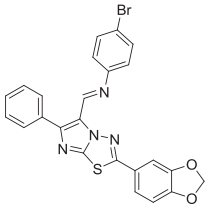	$C_{24}H_{15}BrN_4O_2S$	503.3705	170–173	78
4c	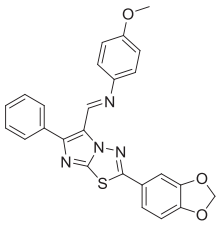	$C_{25}H_{18}N_4O_3S$	454.5004	170–175	62
4d	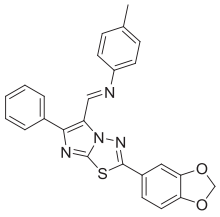	$C_{25}H_{18}N_4O_2S$	438.5010	158–163	56
7a	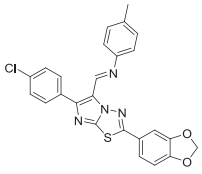	$C_{25}H_{17}ClN_4O_2S$	472.9461	158–162	68
7b	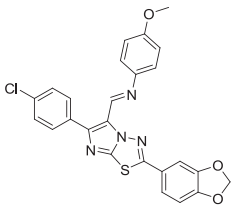	$C_{25}H_{17}ClN_4O_3S$	488.9455	234–239	78
7c	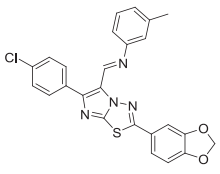	$C_{25}H_{17}ClN_4O_2S$	472.9461	205–210	82

Table 1 (*continued*)

Sr. No.	Compound	Molecular formula	Molecular weight	Melting point (°C)	Yield (%)
7d	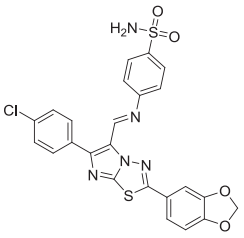	$C_{24}H_{16}ClN_5O_4S_2$	537.9979	223–228	73
7e	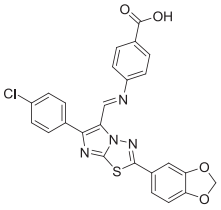	$C_{25}H_{15}ClN_4O_4S$	502.9290	234–238	76
7f	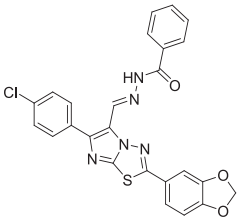	$C_{25}H_{16}ClN_5O_3S$	501.9442	198–201	78
7g	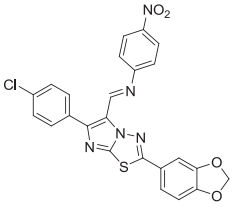	$C_{24}H_{14}ClN_5O_4S$	503.9171	225–228	63
7h	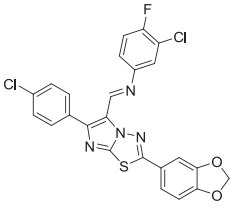	$C_{24}H_{13}Cl_2FN_4O_2S$	511.3550	245–248	69
7i	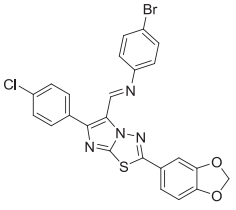	$C_{24}H_{14}BrClN_4O_2S$	537.8156	190–192	64

data bank (PDB ID: 1OSH) [33]. The protein preparation was carried out using 'protein preparation wizard' in Maestro 9.0 in two steps, preparation and refinement. After ensuring chemical correctness, water molecules in the crystal structures were deleted and hydrogens were added, where they were missing. Using the OPLS 2005 force field energy of crystal structure was minimized [34]. Grids were defined centering them on the ligand in the crystal structure using the default box size. The ligands were built using maestro build panel and prepared by Ligprep 2.2 module which produce the low energy conformer of ligands using OPLS 2005 force field. The low energy conformation of the ligands was selected and was docked into the grid generated from protein structures using standard precision (SP) docking mode. The final evaluation is done with glide score (docking score) and single best pose is generated as the output for particular ligand.

6. Results and discussion

The formation of 5-(benzo[*d*][1,3]dioxol-5-yl)-[1,3,4]thiadiazol-2-amine (**1**) was confirmed by IR spectra, which showed the

presence of amine (Ar–NH_2) band and the absence of carbonyl stretching of carboxylic acid. Structures of imidazo thiadiazole derivatives (**2** and **5**) were established by the absence of amine (Ar–NH_2) band in IR spectra and appearance of imidazole proton (H-5) around δ 8.21 and 8.31 in the ^{1}H NMR spectra. IR spectra of aldehydes (**3** and **6**) displayed a sharp band for carbonyl stretching frequency around 1724 cm^{-1} and the signal for imidazole proton (H-5) in ^{1}H NMR spectrum was absent. A new signal for aldehydic proton was observed around δ 10.00 in the ^{1}H NMR spectra, thus substantiating the formation of imidazo[2,1-*b*][1,3,4]thiadiazole-5-carbaldehydes. The absence of aldehydic protons and presence of the imine proton (CH=N) around δ 8.5 in ^{1}H NMR spectra of the product supported the formation of the title compounds **4**(**a**–**d**) and **7**(**a**–**i**). The ^{13}C NMR and HRMS data of these compounds further confirmed the assigned structures.

The main biochemical parameters recommended by the National Cholesterol Education Programme (NCEP) guidelines (2002) for lipid screening i.e. Total Cholesterol (TCH), Triglycerides, Low Density Lipoprotein (LDL), Very Low Density Lipoprotein (VLDL) and High Density Lipoprotein (HDL) were evaluated from the serum Wistar albino rats [35]. The present investigation shows that all triton induced rats displayed hyperlipidemia as shown by their elevated levels of serum cholesterol, triglyceride, VLDL, LDL and the reduction in the HDL level. In cholesterol induced hyperlipidemic model, among **4**(**a**–**d**) and **7**(**a**–**i**) the groups treated with the **7d**, **7e** and **7h** and Fenofibrate demonstrated a significant decrease in the serum TCH, TG, LDL and VLD besides an increase in serum HDL levels when compared to trition induced hyperlipidemic control group (Table 2). The cardiac risk ratios recommended by NCEP guidelines (2002) were estimated by calculating the TCH: HDL ratio (Atherogenic Index) and LDL:HDL ratio [36]. The groups treated with **7d**, **7e** and **7h** also demonstrated significant decrease in atherogenic index and LDL:HDL risk ratios as shown in Table 2. Hepatotoxicity of some potent compounds were further evaluated by measuring alanine transferase, aspartate transferase and alkaline phosphatase levels in serum and a remarkable decrease in the level of SGOT, SGPT and ALP activities when compared to cholesterol induced hyperlipidemic control group (Table 3). In cholesterol induced hyperlipidemic model, the histopathological studies were conducted in the liver section of rats to observe the histopathological changes (Fig. 2). Fig. 2 illustrates the protective action of the synthesized compounds, among them compound **7d**, **7e** and **7h** treated group shows mild cytoplasmic fatty infiltration and mild granular degeneration, on the other hand compound **7h** and **7i** treated group shows mild cytoplasmic fatty infiltration and mild to moderate granular degeneration compared to that of Fenofibrate.

Docking study was carried out for the target compounds into EGFR using GLIDE (Schordinger Inc., USA) (2009). The crystal structure of the enzyme with Fexaramine (PDB: 1OSH) was obtained from protein data bank PDB [33]. Our compounds were modeled by positioning them in the co-crystallized ligand Fexaramine binding site in accordance with the published crystal structures [37]. The entire complex was then subjected to alternate cycles of minimization and dynamics. The intent was to get a satisfactory structure for the complex that was consistent with the published crystal structure [38,39]. From the comparative docking study of our compounds with Fexaramine lead compounds we could observe how our compounds might bind to the FXR binding site, based on the knowledge of the structure of similar active sites. We redocked Fexaramine into the active site of the enzyme and then we replaced with our compounds in order to compare the binding mode of both co-crystallized ligand and the test compound. These docking studies have revealed that the most of the synthesized compounds shows H-bonding with HIE-298 amino acid backbone via *N*-6 of imidazo[2,1-*b*][1,3,4]thiadiazoles. On the other hand imidazo[2,1-*b*][1,3,4]thiadiazoles containing oxygen in the form of sulphonamide, carboxylic acid, amide and nitro group shows H-bonding interaction with backbone of HIE-298 and SER-336. These interactions underscore the importance of both nitrogen and oxygen as hydrogen bond acceptor for binding and the subsequent agonistic capacity. The results of this virtual screening could support the postulation that our active compounds may bind on the same enzyme target where Fexaramine binds. With respective to the glide score Compound **7e**, **7d** and **7f** shows highest binding affinity with glide score of −9.89, −9.24 and −8.32 kcal/mol indicating the importance of oxygen as hydrogen bond acceptor as shown in Table 4 and Fig. 3.

7. Structure activity relationship

A brief investigation of the structure–activity relationship (SAR) revealed that the compounds with 4-choloro phenyl substitution at 6th position of imidazo[2,1-*b*][1,3,4]thiadiazole nucleus is more potent than the plane phenyl substitution as it is obvious by comparing in vitro antihyperlipidemic activity of **7**(**a**–**i**) and **4**(**a**–**d**). In case of compound **7**(**a**–**i**), the derivatives with electron withdrawing substituent at 5th position of imidazo[2,1-*b*][1,3,4] thiadiazole, found to significantly affect over the lipid parameters (**7e**, **7g**, **7h** and **7i**). On the other hand electron-donating substituent at 5th position is having diminishing effect on biological activity (Compound **4d**, **7a** and **7c**).

8. Conclusion

A new series of 2,5,6-trisubstituted imidazo[2,1-*b*][1,3,4]thiadiazoles **4**(**a**–**d**) and **7**(**a**–**i**) were rationally designed through QSAR base pharmacophore approach. All the compounds were evaluated for their in vitro antihyperlipidemic activity, among them **7d**, **7e** and **7h** showed a significant decrease in the serum, TC, LDL, VLDL and TG values along with an increase in serum HDL levels as compared to standard drug Fenofibrate. The treated groups also showed significant decrease in the atherogenic index, LDL:HDL risk ratios which are a reliable risk assessment factor of coronary heart disease. Hepatotoxicity was evaluated by measuring alanine transferase, aspartate transferase and alkaline phosphatase levels in serum and no compound was found to be hepatotoxic. Possible improvements in the antihyperlipidemic activity can be further achieved by slight modifications in the substituent's and/or additional structural activity investigations. These preliminary encouraging results of biological screening of the tested compounds could offer an excellent framework in this field that may lead to discovery of potent antihyperlipidemic agent.

9. Experimental protocols

All chemicals and solvents were supplied by Merck, S.D. Fine Chemical Limited, Mumbai. All the solvents were distilled and dried before use. The reactions were monitored with the help of thin-layer chromatography using pre-coated aluminum sheets with GF_{254} silica gel, 0.2 mm layer thickness (E. Merck). The solvents used throughout the experiment for running TLC were toluene, ethyl acetate and formic acid in the ratio of 5:4:1, chloroform and methanol in the ratio of 9.5:0.5 and 9:1 as developing solvents. UV Cabinet was used for the visualization of TLC spots. Melting points of the synthesized compounds were recorded on the Veego (VMP-MP) melting point apparatus. IR spectrum was acquired on a Shimadzu Infra Red Spectrometer, (model FTIR-8400S). Both ^{1}H NMR (DMSO) and ^{13}C NMR (DMSO) spectra of the synthesized compounds were performed with Bruker Avance-II 400 NMR Spectrometer operating at 400 MHz in SAIF, Punjab University

Table 2
Data of total lipid profile (TCH, TG, VLDL, LDL and HDL).

Compound code	Compound	Parameter (mg/dl)					Atherogenic index	LDL/HDL
		TCH	TG	VLDL	LDL	HDL	TCH/HDL	
Normal		71.17 ± 0.612	76.19 ± 0.718	14.03 ± 0.689	21.19 ± 0.721	36.5 ± 0.821	1.94	0.58
Positive Control		126.5 ± 1.234[a]	138 ± 1.345[a]	29 ± 0.3781[a]	78.5 ± 1.623[a]	16 ± 0.4213[a]	7.90	4.90
Standard	Fenofibrate	102.24 ± 1.561[a]	71.23 ± 1.678[a]	13.67 ± 0.234[a]	51.68 ± 0.978[a]	35.21 ± 0.321[a]	2.90	1.46
4a	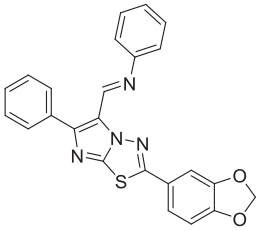	118.23 ± 1.563[a]	89.12 ± 1.543[a]	21.54 ± 0.231[a]	65.85 ± 1.432[a]	25.12 ± 0.8322[a]	4.70	2.62
4b	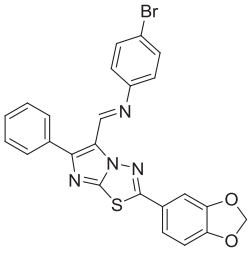	112.78 ± 1.853[a]	86.89 ± 1.645[a]	19.86 ± 0.121[a]	63.74 ± 0.231[a]	24.78 ± 0.2432[a]	4.55	2.57
4c	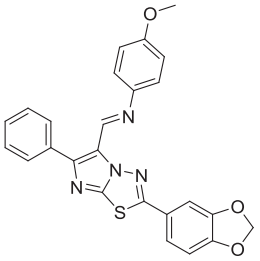	113.98 ± 0.986[a]	84.98 ± 1.235[a]	18.46 ± 0.134[a]	64.73 ± 0.837[a]	28.83 ± 0.7822[a]	3.95	2.24
4d	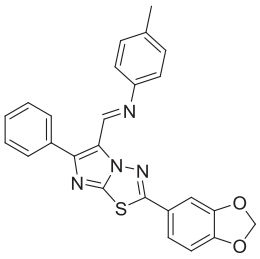	114.36 ± 0.882[a]	88.43 ± 2.231[a]	22.83 ± 0.285[a]	66.32 ± 1.384	23.34 ± 0.7349[a]	4.89	2.84
7a	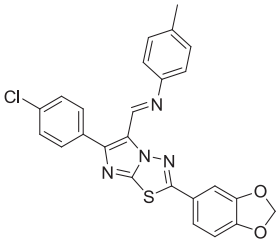	113.28 ± 1.213[b]	85.67 ± 1.632[a]	18.35 ± 0.345[a]	68.84 ± 1.394[a]	29.12 ± 0.6783[c]	3.89	2.36
7b	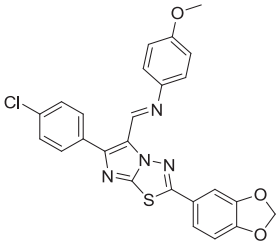	107.83 ± 1.736[a]	83.56 ± 1.674[a]	16.86 ± 0.563[a]	59.85 ± 2.129[a]	31.34 ± 0.7839[a]	3.44	1.90

(*continued on next page*)

Table 2 (*continued*)

Compound code	Compound	Parameter (mg/dl)					Atherogenic index	LDL/HDL
		TCH	TG	VLDL	LDL	HDL	TCH/HDL	
7c	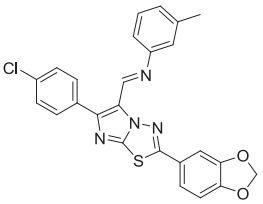	113.72 ± 0.728[b]	86.23 ± 1.523[a]	19.93 ± 0.472[a]	62.83 ± 1.098[a]	28.12 ± 0.5648[a]	4.04	2.23
7d	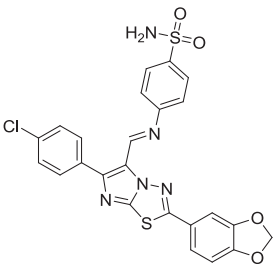	101.56 ± 1.483[a]	79.54 ± 1.356[a]	14.73 ± 0.365[a]	52.23 ± 1.838[a]	33.78 ± 0.5732[a]	3.00	1.54
7e	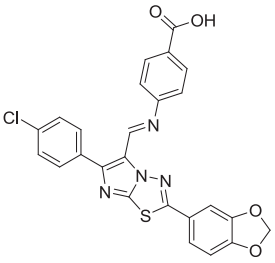	96.12 ± 1.891[a]	76.89 ± 1.457[a]	15.85 ± 0.657[a]	49.94 ± 2.243[a]	34.78 ± 0.5428[a]	2.76	1.43
7f	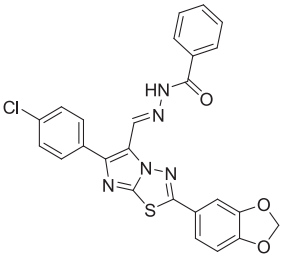	107.87 ± 0.643[a]	80.67 ± 2.124[a]	16.34 ± 0.345[a]	59.12 ± 1.839[a]	29.93 ± 0.6231[a]	3.60	1.97
7g	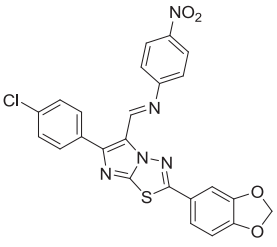	105.56 ± 1.342[a]	82.56 ± 1.674[a]	18.13 ± 0.9678[a]	58.24 ± 1.782[a]	31.54 ± 0.1464[a]	3.34	1.84
7h	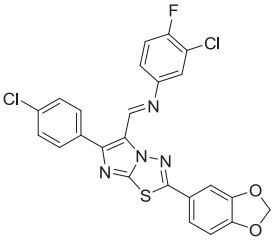	99.89 ± 0.543[a]	80.45 ± 1.853	15.43 ± 0.232[a]	54.95 ± 1.637[a]	33.57 ± 0.6723[a]	2.97	1.63

Table 2 (*continued*)

Compound code	Compound	Parameter (mg/dl)					Atherogenic index	LDL/HDL
		TCH	TG	VLDL	LDL	HDL	TCH/HDL	
7i	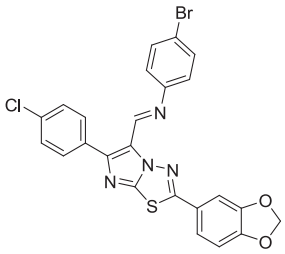	103.54 ± 1.367[a]	83.43 ± 1.673	16.85 ± 0.466[a]	53.82 ± 2.45[a]	32.85 ± 0.1643[a]	3.15	1.63

Test compounds = 250 mg/kg, reference standard, Fenofibrate = 250 mg/kg, The results are expressed as mean ± SEM, ($n = 6$). The data is analyzed by using one-way analysis of variance (ANOVA) followed by Turkey's test.

[a] $p < 0.001$.

[b] $p < 0.01$.

[c] Non significant.

(Chandigarh). Chemical shifts were measured relative to internal standard TMS (δ: 0). Chemical shifts are reported in δ scale (ppm). Mass spectra of the synthesized compounds were recorded at MAT 120 in SAIF, Punjab University.

9.1. 5-(Benzo[d][1,3]dioxol-5-yl)-[1,3,4]thiadiazol-2-amine (**1**)

It is prepared as per the procedure given by G. Tu et al. [22].

9.2. 2-(Benzo[d][1,3]dioxol-5-yl)-6-phenylimidazo[2,1-b][1,3,4] thiadiazole (**2**) and 2(benzo[d][1,3]dioxol-5-yl)-6-phenylimidazo [2,1-b][1,3,4]thiadiazole-5-carbaldehyde (**3**)

It is prepared as per the procedure given by G. Kolavi et al. [23].

9.3. General procedure for preparation of N-((2-(benzo[d][1,3] dioxol-5-yl)-6-phenylimidazo[2,1-b][1,3,4]thiadiazol-5-yl) methylene)-substituted anilines **4**(**a**–**d**)

Equimolar quantities of 2-(benzo[*d*][1,3]dioxol-5-yl)-6-phenylimidazo[2,1-*b*][1,3,4]thiadiazole-5-carbaldehyde **3** (0.01 M) and substituted anilines (0.01 M) in 40 mL of ethanol was taken in 100 mL of round bottomed flask fitted with condenser. The mixture was heated under reflux using water bath. When the solution is mixed then added 1–2 drops of glacial acetic acid then reflux for 6 h, the reaction mixture was set aside for cooling. The solid deposit was collected by filtration. The product was recrystallized from ethanol.

9.3.1. N-((2-(Benzo[d][1,3]dioxol-5-yl)-6-phenylimidazo[2,1-b] [1,3,4]thiadiazol-5-yl)methylene) aniline (**4a**)

IR (KBr) ν_{max} 3067 (CH), 1648 (C=N), 1582 (C=C), 1282 (C–O) cm^{-1}; ^{1}H NMR (DMSO-d_6) δ ppm: 8.56 (s, 1H, CH=N), 6.89–7.89 (m, 13H, Ar–H), 6.01 (s, 2H, CH_2, benzo-1,3-dioxole); ^{13}C NMR (DMSO-d_6) δ ppm: 150.2, 148.6, 145.8, 121.4 (imidazo[2,1-*b*][1,3,4] thiadiazole) 153.1, 151.6, 128.8, 123.8, 115.2, 112.5, 102.6 [2-(1,3-benzodioxol-5-yl)] 153.9, 131.2, 129.3, 127.2, 113.5 (5-methylidene aniline) 138.6, 135.8, 131.0, 130.6 (6-phenyl); HRMS (EI) *m*/*z* calcd for $C_{24}H_{16}N_4O_2S$: 424.0994; found: 424.0997.

9.3.2. N-((2-(Benzo[d][1,3]dioxol-5-yl)-6-phenylimidazo[2,1-b] [1,3,4]thiadiazol-5-yl) methylene)-4-bromoaniline (**4b**)

IR (KBr) ν_{max} 3050 (CH), 1652 (C=N), 1506 (C=C), 1278 (C–O), 634 (C–Br) cm^{-1}; ^{1}H NMR (DMSO-d_6) δ ppm: 8.48 (s, 1H, CH=N), 6.91–7.85 (m, 12H, Ar–H), 6.07 (s, 2H, CH_2, benzo-1,3-dioxole); ^{13}C NMR (DMSO-d_6) δ ppm: 149.8, 148.3, 145.4, 121.5 (imidazo [2,1-*b*][1,3,4]thiadiazole) 153.4, 151.2, 129.5, 122.8, 117.6, 112.6, 102.8 [2-(1,3-benzodioxol-5-yl)] 150.6, 135.8, 127.6, 123.4, 113.8 (5-methylidene aniline) 138.6, 133.2, 131.2, 129.5 (6-phenyl); HRMS (EI) *m*/*z* calcd for $C_{24}H_{15}BrN_4O_2S$: 502.0099; found: 502.0097.

9.3.3. N-((2-(Benzo[d][1,3]dioxol-5-yl)-6-phenylimidazo[2,1-b] [1,3,4]thiadiazol-5-yl) methylene)-4-methoxyaniline (**4c**)

IR (KBr) ν_{max} 3042 (CH), 1672 (C=N), 1564 (C=C), 1178 (C–O) cm^{-1}; ^{1}H NMR (DMSO-d_6) δ ppm: 8.64 (s, 1H, CH=N), 6.95–8.20 (m, 12H, Ar–H), 6.09 (s, 2H, CH_2, benzo-1,3-dioxole), 3.90 (s, 1H, OCH_3); ^{13}C NMR (DMSO-d_6) δ ppm: 150.5, 145.8, 145.2, 121.6 (imidazo[2,1-*b*][1,3,4]thiadiazole) 153.6, 151.6, 129.4, 127.4, 115.4, 110.8, 102.4 [2-(1,3-benzodioxol-5-yl)] 160.4, 148.4, 123.6, 116.4, 112.4 (5-methylidene aniline) 138.2, 135.8, 131.6, 130.4 (6-phenyl) 56.4 (OCH_3); HRMS (EI) *m*/*z* calcd for $C_{25}H_{18}N_4O_3S$: 454.1100; found: 454.1103.

9.3.4. N-((2-(Benzo[d][1,3]dioxol-5-yl)-6-phenylimidazo[2,1-b] [1,3,4]thiadiazol-5-yl) methylene)-4-methylaniline (**4d**)

IR (KBr) ν_{max} 3011 (CH), 1652 (C=N), 1521 (C=C), 1265 (C–O) cm^{-1}; ^{1}H NMR (DMSO-d_6) δ ppm: 8.56 (s, 1H, CH=N), 6.92–7.88 (m, 12H, Ar–H), 6.04 (s, 2H, CH_2, benzo-1,3-dioxole), 2.61 (s, 3H, CH_3); ^{13}C NMR (DMSO-d_6) δ ppm: 150.4, 146.6, 138.4, 121.4 (imidazo [2,1-*b*][1,3,4]thiadiazole) 153.6, 151.2, 129.6, 123.1, 117.4, 112.0, 102.8 [2-(1,3-benzodioxol-5-yl)] 148.4, 145.6, 135.7, 127.6, 113.4 (5-methylidene aniline) 138.1, 131.2, 131.0, 130.0 (6-phenyl) 24.8 (CH_3); HRMS (EI) *m*/*z* calcd for $C_{25}H_{18}N_4O_2S$: 438.1150; found: 438.1153.

9.4. Synthesis of 2-(benzo[d][1,3]dioxol-5-yl)-6-(4-chlorophenyl)imidazo[2,1-b][1,3,4]thiadiazole (**5**) and 2-(benzo[d][1,3]dioxol-5-yl)-6-(4-chlorophenyl)imidazo[2,1-b][1,3,4]thiadiazole-5-carbaldehyde (**6**)

It is prepared as per the procedure given by G. Kolavi et al. [27].

9.5. General procedure for preparation N-((2-(benzo[d][1,3]dioxol-5-yl)-6-(4-chlorophenyl)imidazo[2,1-b][1,3,4]thiadiazol-5-yl)methylene)substituted aniline **7**(**a**–**i**)

Equimolar quantities of 2-(benzo[*d*][1,3]dioxol-5-yl)-6-(4-chlorophenyl)imidazo[2,1-*b*][1,3,4]thiadiazole-5-carbaldehyde **6**

Table 3
Effect of synthesized compounds **7d, 7e**, **7g**, **7h** and **7i** on liver marker enzyme.

Compound code	Compound	Alanine transferase (SGPT) IU	Aspartate transferase (SGOT) IU	Alkaline phosphatase KA unit
Normal range		18–30	46–81	14–32
Normal control		24.2 ± 1.0[a]	48.4 ± 2.1[a]	28.8 ± 1.5[a]
Hyperlipidemic control		42.32 ± 0.54	85.84 ± 1.12	41.64 ± 1.65
Fenofibrate treated		26.43 ± 1.21[a]	49.45 ± 1.34[a]	28.33 ± 0.43[a]
Compound **7d**	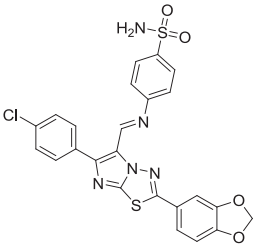	28.6 ± 0.5[a]	51.7 ± 1.5[a]	29.3 ± 0.3[a]
Compound **7e**	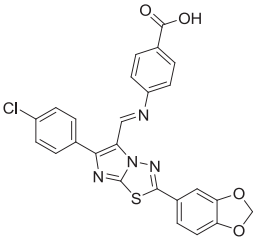	26.8 ± 0.5[a]	48.3 ± 1.8[a]	29.5 ± 0.5[a]
Compound **7g**	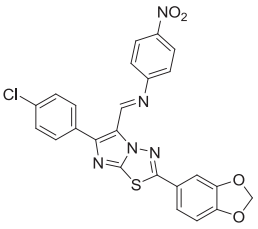	28.3 ± 1.0[a]	49.9 ± 2.3[a]	28.8 ± 1.2[a]
Compound **7h**	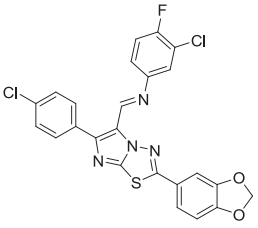	27.8 ± 1.0[a]	56.5 ± 2.1[a]	27.3 ± 1.0[a]
Compound **7i**	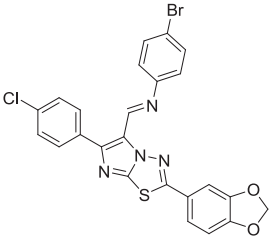	29.3 ± 0.5[a]	58.8 ± 1.2[a]	26.6 ± 0.5[a]

The results are expressed as mean ± SEM, ($n = 6$). The data is analyzed by using one-way analysis of variance (ANOVA) followed by Turkey's test.
[a] $p < 0.001$.

(0.01 M) and substituted amines (0.01 M) in 40 mL of ethanol was taken in 100 mL of round bottomed flask fitted with condenser. The mixture was heated under reflux using water bath. When the solution is mixed then added 1–2 drops of glacial acetic acid then reflux for 6 h, the reaction mixture was set aside for cooling. The solid deposit was collected by filtration. The product was recrystallized from ethanol.

*9.5.1. N-((2-(Benzo[d][1,3]dioxol-5-yl)-6-(4-chlorophenyl)imidazo [2,1-b][1,3,4]thiadiazol-5-yl)methylene)-4-methylaniline (**7a**)*

IR (KBr) ν_{max} 3026 (CH), 1645 (C=N), 1556 (C=C), 1261 (C–O), 710 (C–Cl) cm^{-1}; ^1H NMR (DMSO-d_6) δ ppm: 8.56 (s, 1H, CH=N), 6.98–7.88 (m, 11H, Ar–H), 6.16 (s, 2H, CH_2, benzo-1,3-dioxole), 2.62 (s, 3H, CH_3); ^{13}C NMR (DMSO-d_6) δ ppm: 150.4, 145.6, 136.4, 122.4 (imidazo [2,1-*b*][1,3,4]thiadiazole) 153.2, 151.4, 129.4, 124.6, 118.5 [2-(1,3-

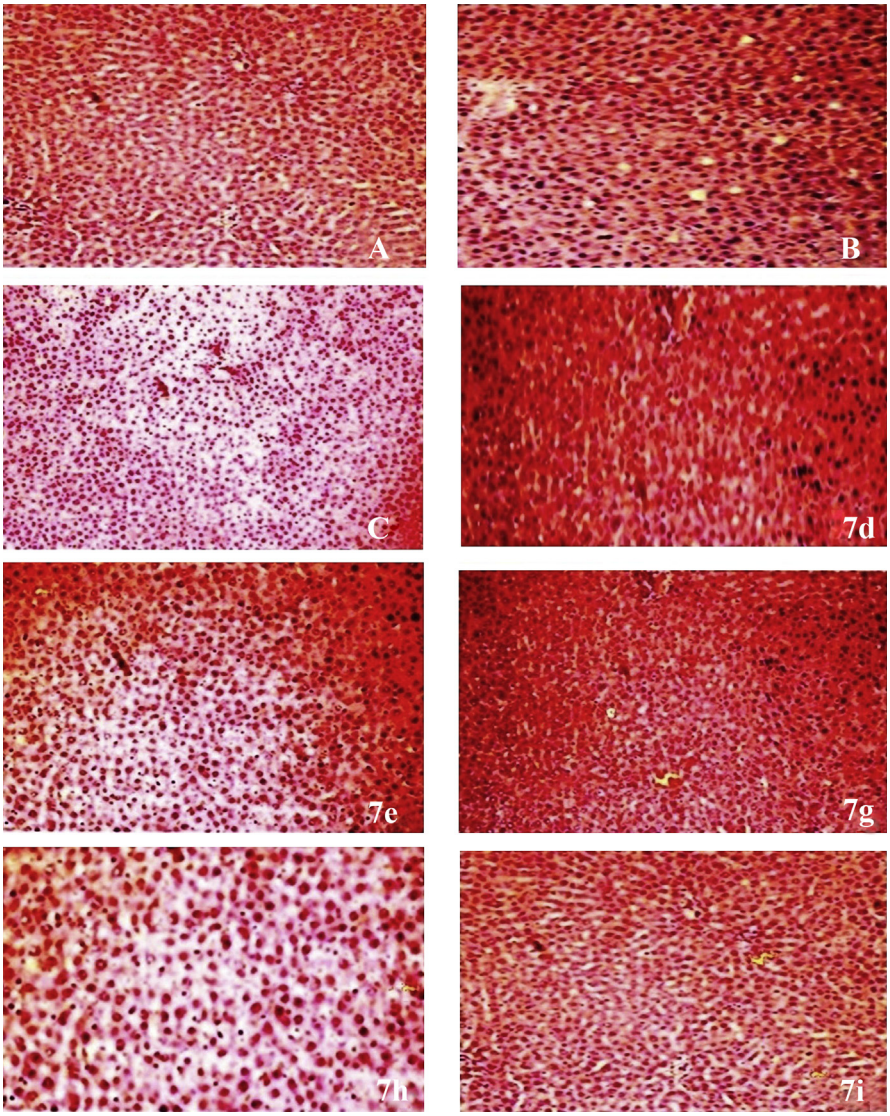

Fig. 2. Hepatocytes of rats stained with hematoxylin and eosin (100× magnification); a) control group showing normal architecture; b) hyperlipidemic group showing fatty infiltration and granular degeneration; c) Fenofibrate group showing negligible cytoplasmic fatty infiltration and granular degeneration; d) compound **7d**, **7e** and **7h** treated group showing mild cytoplasmic fatty infiltration and mild granular degeneration; e) compound **7g** and **7i** treated group showing mild cytoplasmic fatty infiltration and mild to moderate granular degeneration.

benzodioxol-5-yl)] 148.4, 144.8, 131.5, 128.6, 114.2 (5-methylidene aniline) 135.8, 134.5, 132.8, 130.8 (6-phenyl) 24.3 (CH_3); HRMS (EI) *m*/*z* calcd for $C_{25}H_{17}ClN_4O_2S$: 472.0761; found: 472.0763.

*9.5.2. N-((2-(Benzo[d][1,3]dioxol-5-yl)-6-(4-chlorophenyl)imidazo [2,1-b][1,3,4]thiadiazol-5-yl)methylene)-3-methoxyaniline (**7b**)*

IR (KBr) ν_{max} 3078 (CH), 1656 (C═N), 1511 (C═C), 1249 (C–O), 721 (C–Cl) cm^{-1}; ^1H NMR (DMSO-d_6) δ ppm: 8.35 (s, 1H, CH═N), 7.02–7.91 (m, 11H, Ar–H), 6.19 (s, 2H, CH_2, benzo-1,3-dioxole), 3.91 (s, 3H, OCH_3); ^{13}C NMR (DMSO-d_6) δ ppm: 150.2, 148.8, 145.4, 122.3 (imidazo[2,1-*b*][1,3,4]thiadiazole) 152.5, 151.6, 128.6, 127.5, 116.3, 112.4, 102.4 [2-(1,3-benzodioxol-5-yl)] 164.6, 153.6, 131.6, 118.2, 114.2, 110.6, 108.6 (5-methylidene aniline) 136.6, 135.4, 132.6, 130.2 (6-phenyl) 56.2 (OCH_3); HRMS (EI) *m*/*z* calcd for $C_{25}H_{17}ClN_4O_3S$: 488.0710; found: 488.0713.

*9.5.3. N-((2-(Benzo[d][1,3]dioxol-5-yl)-6-(4-chlorophenyl)imidazo [2,1-b][1,3,4]thiadiazol-5-yl)methylene)-3-methylaniline (**7c**)*

IR (KBr) ν_{max} 3062 (CH), 1634 (C═N), 1580 (C═C), 1261 (C–O),715 (C–Cl) cm^{-1}; ^1H NMR (DMSO-d_6) δ ppm: 8.75 (s, 1H, CH═N), 6.94–7.79 (m, 11H, Ar–H), 6.10 (s, 2H, CH_2, benzo-1,3-dioxole), 2.64 (s, 3H, CH_3); ^{13}C NMR (DMSO-d_6) δ ppm: 150.1, 148.6, 141.4, 116.2 (imidazo[2,1-*b*][1,3,4]thiadiazole) 153.4, 150.3, 129.9, 122.6, 114.2, 110.3, 102.4 [2-(1,3-benzodioxol-5-yl)] 151.8, 145.2, 132.6, 126.6, 124.6, 120.6, 112.4 (5-methylidene aniline) 136.2, 135.2, 133.6, 130.4 (6-phenyl) 24.6 (CH_3); HRMS (EI) *m*/*z* calcd for $C_{25}H_{17}ClN_4O_2S$: 472.0761; found: 472.0764.

*9.5.4. 4-((2-(Benzo[d][1,3]dioxol-5-yl)-6-(4-chlorophenyl)imidazo [2,1-b][1,3,4]thiadiazol-5-yl)methyleneamino)benzenesulfonamide (**7d**)*

IR (KBr) ν_{max} 3448 (NH), 3011 (CH), 1676 (C═N), 1581 (C═C), 1248 (C–O), 661 (C–Cl) cm^{-1}; ^1H NMR (DMSO-d_6) δ ppm: 8.32 (s, 1H, CH═N), 6.89–7.92 (m, 11H, Ar–H), 6.09 (s, 2H, CH_2, benzo-1,3-dioxole), 4.01 (s, 2H, NH_2) ^{13}C NMR (DMSO-d_6) δ ppm: 150.6, 146.3, 143.4, 124.4 (imidazo[2,1-*b*][1,3,4]thiadiazole) 152.9, 151.6, 127.4, 122.4, 114.6, 111.2, 106.3 [2-(1,3-benzodioxol-5-yl)] 153.2, 145.3, 130.4, 128.4, 116.2 (5-methylidene aniline) 136.2, 135.6, 133.4, 132.4 (6-phenyl); HRMS (EI) *m*/*z* calcd for $C_{24}H_{16}ClN_5O_4S_2$: 537.0332; found: 537.0335.

Table 4
Glide docking results based on hydrogen bonding interaction, glide dock score and E-model.

Compound Code	Compound	H-bond interaction	Glide score (kcal/mol)	E-model
Compound **4a**	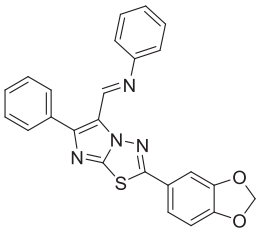	N-6 of imidazo[2,1-*b*][1,3,4]thiadiazoles and H atom of amino acid backbone of HIE-298	−4.84	−76.67
Compound **4b**	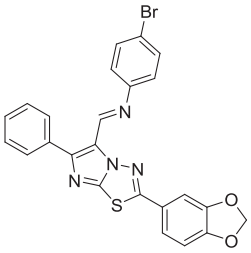	N-6 of imidazo[2,1-*b*][1,3,4]thiadiazoles and H atom of amino acid backbone of HIE-298	−5.34	−80.45
Compound **4c**	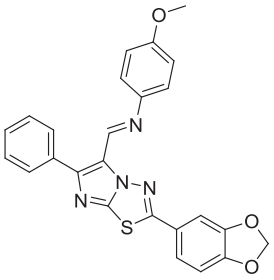	N-6 of imidazo[2,1-*b*][1,3,4]thiadiazoles and H atom of amino acid backbone of HIE-298	−6.88	−83.34
Compound **4d**	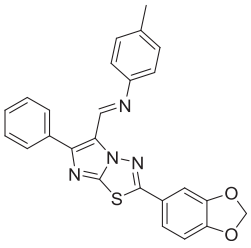	N-6 of imidazo[2,1-*b*][1,3,4]thiadiazoles and H atom of amino acid backbone of HIE-298	−4.48	−74.74
Compound **7a**	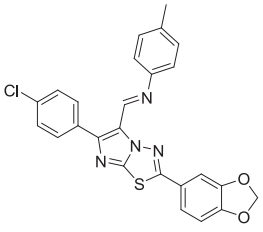	N-6 of imidazo[2,1-*b*][1,3,4]thiadiazoles and H atom of amino acid backbone of HIE-298	−4.68	−75.21
Compound **7b**	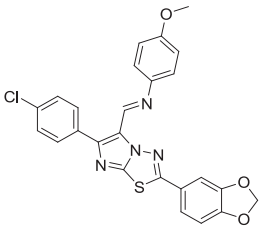	N-6 of imidazo[2,1-*b*][1,3,4]thiadiazoles and H atom of amino acid backbone of HIE-298	−5.88	−79.43

Table 4 (*continued*)

Compound Code	Compound	H-bond interaction	Glide score (kcal/mol)	E-model
Compound **7c**	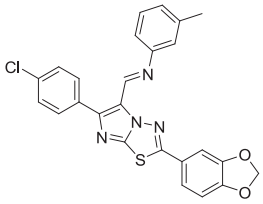	N-6 of imidazo[2,1-*b*][1,3,4]thiadiazoles and H atom of amino acid backbone of HIE-298	−4.34	−73.74
Compound **7d**	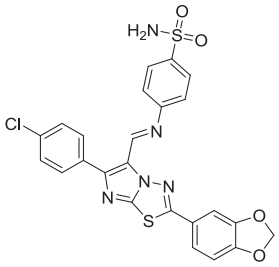	Oxygen of sulphonamido group and H atom of amino acid backbone of HIE-298 and SER-336	−9.24	−96.56
Compound **7e**	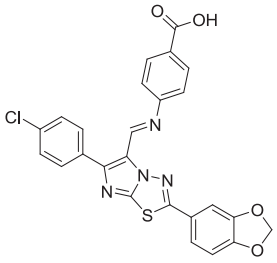	Oxygen of carboxyl group and H atom of amino acid backbone of HIE-298 and SER-336	−9.89	−98.88
Compound **7f**	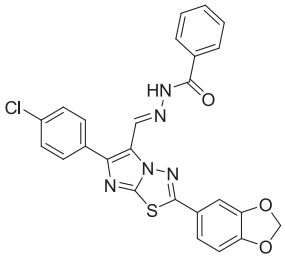	Oxygen of amide group and H atom of amino acid backbone of HIE-298 and SER-336	−8.32	−82.82
Compound **7g**	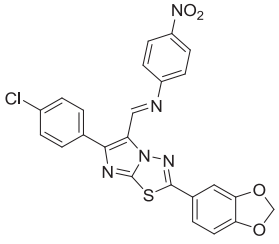	Oxygen of nitro group and H atom of amino acid backbone of HIE-298 and SER-336	−8.21	−84.99
Compound **7h**	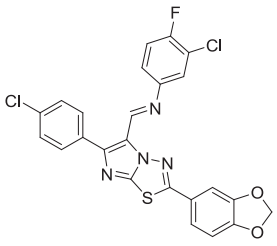	N-6 of imidazo[2,1-*b*][1,3,4]thiadiazoles and H atom of amino acid backbone of HIE-298	−8.01	−81.24

(*continued on next page*)

Table 4 (*continued*)

Compound Code	Compound	H-bond interaction	Glide score (kcal/mol)	E-model
Compound **7i**	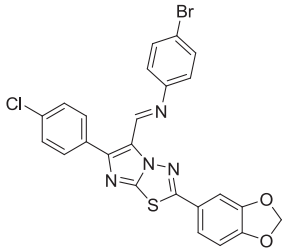	N-6 of imidazo[2,1-*b*][1,3,4]thiadiazoles and H atom of amino acid backbone of HIE-298	−6.78	−80.82

*9.5.5. 4-((2-(Benzo[d][1,3]dioxol-5-yl)-6-(4-chlorophenyl)imidazo [2,1-b][1,3,4]thiadiazol-5-yl)methyleneamino)benzoic acid (**7e**)*

IR (KBr) ν_{max} 3450 (OH), 3009 (CH), 1672 (C═N), 1584 (C═C), 1259 (C–O), 708 (C–Cl) cm^{-1}; ^1H NMR (DMSO-d_6) δ ppm: 10.56 (s, 1H, COOH), 8.62 (s, 1H, CH═N), 6.90–8.03 (m, 11H, Ar–H), 6.14 (s, 2H, CH_2, benzo-1,3-dioxole),; ^{13}C NMR (DMSO-d_6) δ ppm: 150.2, 148.4, 144.6, 122.8 (imidazo[2,1-*b*][1,3,4]thiadiazole) 153.2, 151.5, 129.4, 124.5, 124.5, 116.8, 110.8, 102.4 [2-(1,3-benzodioxol-5-yl)] 170.1, 155.6, 132.6, 129.6, 127.8, 112.6 (5-methylidene aniline) 136.8, 135.7, 133.7, 130.2 (6-phenyl); HRMS (EI) *m/z* calcd for $C_{25}H_{15}ClN_4O_4S$: 502.0503; found: 502.0505.

*9.5.6. N′-((2-(Benzo[d][1,3]dioxol-5-yl)-6-(4-chlorophenyl)imidazo [2,1-b][1,3,4]thiadiazol-5-yl)methylene)benzohydrazide (**7f**)*

IR (KBr) ν_{max} 3448 (NH), 3031 (CH), 1656 (C═O),1671 (C═N), 1515 (C═C), 1271 (C–O),689 (C–Cl) cm^{-1}; ^1H NMR (DMSO-d_6) δ ppm: 8.79 (s, 1H, CH═N), 6.93–8.04 (13H, Complex containing Ar–H and NH), 6.12 (s, 2H, CH_2, benzo-1,3-dioxole); ^{13}C NMR (DMSO-d_6) δ ppm: 148.9, 145.6, 141.3, 116.4 (imidazo[2,1-*b*][1,3,4] thiadiazole) 151.2, 150.4, 127.6, 122.4, 114.6, 112.4, 102.4 [2-(1,3-benzodioxol-5-yl)] 165.4, 135.5, 133.2, 129.3, 128.4, 110.3 (5-methylidene aniline) 136.6, 133.6, 132.6, 130.6 (6-phenyl); HRMS (EI) *m/z* calcd for $C_{25}H_{16}ClN_5O_3S$: 501.0662; found: 501.0662.

*9.5.7. N-((2-(Benzo[d][1,3]dioxol-5-yl)-6-(4-chlorophenyl)imidazo [2,1-b][1,3,4]thiadiazol-5-yl)methylene)-4-nitroaniline (**7g**)*

IR (KBr) ν_{max} 3061 (CH), 1678 (C═N), 1581 (C═C), 1551, 1342 (NO_2), 1249 (C–O), 705 (C–Cl) cm^{-1}; ^1H NMR (DMSO-d_6) δ ppm: 8.62 (s, 1H, CH═N), 7.01–8.12 (m, 11H, Ar–H), 6.11 (s, 2H, CH_2, benzo-1,3-dioxole); ^{13}C NMR (DMSO-d_6) δ ppm: 148.4, 147.2, 145.4, 122.4 (imidazo[2,1-*b*][1,3,4]thiadiazole) 153.6, 151.8, 130.2, 124.5, 116.2, 112.4, 102.4 [2-(1,3-benzodioxol-5-yl)] 158.4, 150.4, 128.6, 126.6, 114.2 (5-methylidene aniline) 136.1, 135.6, 133.4, 132.4 (6-phenyl); HRMS (EI) *m/z* calcd for $C_{24}H_{14}ClN_5O_4S$: 503.0455; found: 503.0458.

*9.5.8. N-((2-(Benzo[d][1,3]dioxol-5-yl)-6-(4-chlorophenyl)imidazo [2,1-b][1,3,4]thiadiazol-5-yl)methylene)-3-chloro-4-fluoroaniline (**7h**)*

IR (KBr) ν_{max} 3018 (CH), 1659 (C═N), 1535 (C═C), 1254 (C–O), 1084 (C–F), 721 (C–Cl) cm^{-1}; ^1H NMR (DMSO-d_6) δ ppm: 8.71 (s, 1H, CH═N), 6.99–8.04 (m, 10H, Ar–H), 6.15 (s, 2H, CH_2, benzo-1,3-

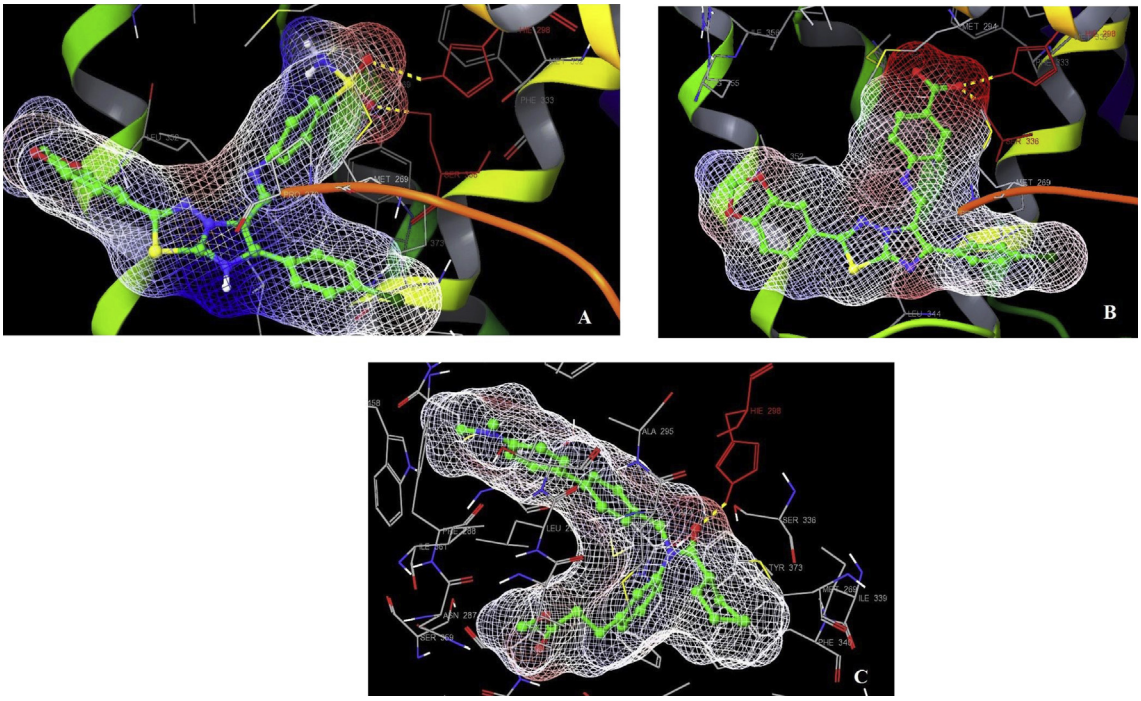

Fig. 3. Binding mode of **7d**, **7e** and co-crystallized ligand Fexaramine in the FXR binding pocket (PDB: 1OSH). Compound **7d** shows H-bond interaction between oxygen of sulphonamido group and compound **7e** shows H-bond interaction between oxygen of carboxyl group with Histidine-298 and Serine-336 amino acid backbone of FXR (Figure A and B), similarly Co-crystallized ligand Fexaramine shows H-bond interaction between oxygen of carboxamide group with Hiestedine-298 backbone of FXR (Figure C).

dioxole); ^{13}C NMR (DMSO-d_6) δ ppm: 149.4, 148.4, 145.8, 116.8 (imidazo[2,1-*b*][1,3,4]thiadiazole) 152.6, 151.6, 130.6, 120.6, 112.3, 111, 101.2 [2-(1,3-benzodioxol-5-yl)] 159.4, 156.4, 127.8, 124.8, 122.6, 118.4, 112.6 (5-methylidene aniline) 136.6, 135.6, 133.6, 132.8 (6-phenyl); HRMS (EI) *m*/*z* calcd for $C_{24}H_{13}Cl_2FN_4O_2S$: 510.0120; found: 510.0123.

*9.5.9. N-((2-(Benzo[d][1,3]dioxol-5-yl)-6-(4-chlorophenyl)imidazo [2,1-b][1,3,4]thiadiazol-5-yl)methylene)-4-bromoaniline (**7i**)*

IR (KBr) ν_{max} 3034 (CH), 1671 (C═N), 1551 (C═C), 1249 (C–O), 705 (C–Cl), 651 (C–Br) cm^{-1}; ^{1}H NMR (DMSO-d_6) δ ppm: 8.74 (s, 1H, CH═N), 6.91–7.95 (m, 11H, Ar–H), 6.12 (s, 2H, CH_2, benzo-1,3-dioxole); ^{13}C NMR (DMSO-d_6) δ ppm: 148.8, 148.1, 145.6, 121.8 (imidazo[2,1-*b*][1,3,4]thiadiazole) 153.4, 151.6, 130.6, 122.7, 116.8, 111.3, 102.8 [2-(1,3-benzodioxol-5-yl)] 150.6, 135.8, 128.8, 124.6, 114.8 (5-methylidene aniline) 136.2, 133.6, 132.6, 131.8 (6-phenyl); HRMS (EI) *m*/*z* calcd for $C_{24}H_{14}BrClN_4O_2S$: 535.9709; found: 535.9711.

Acknowledgment

The authors would like to thank Director General, Department of Science and Technology, New Delhi for funding the project (Grant No. SR/FT/LS-0024/2008).

References

[1] T. Pallavi, P. Anju, C. Ramesh, B. Geetika, Bioorg. Med. Chem. Lett. 16 (2006) 6028–6033.
[2] D.J. Gordon, B.M. Rifkind, N. Engl. J. Med. 321 (1989) 1311–1316.
[3] P.J. Barter, K.A. Rye, Atheresclerosis 121 (1996) 1–12.
[4] D.J. Gordon, J.L. Probsteld, R.J. Garrison, J.D. Neaton, W.P. Castelli, J.D. Knoke, D.R. JacoDbs, S. Bangdiwala, H.A. Tyroler, Circulation 79 (1989) 8–15.
[5] P.C. Ochani, P. D'Mello, Ind. J. Exp. Biol. 47 (2009) 276–282.
[6] M.G. Mamolo, L. Vio, E. Banfi, Farmaco 51 (1996) 71–74.
[7] A.K. Gadad, C.S. Mahajanshetti, S. Nimbalkar, A. Raichurkar, Eur. J. Med. Chem. 35 (2000) 853–857.
[8] E.O. Eclin, R. Sevim, K. Fatma, S. Nathaly, S.D. Anatholy, J. Med. Chem. 47 (2004) 676–684.
[9] A.K. Gadad, M.N. Noolvi, V.K. Rajshekhar, Bioorg. Med. Chem. 12 (2004) 5651–5661.
[10] M.D. Mullican, M.W. Wilson, D.T. Connor, C.R. Kostlan, D.J. Schrier, R.D. Dyer, J. Med. Chem. 36 (1993) 1090–1099.
[11] Y. Song, D.T. Connor, A.D. Sercel, R.J. Soreson, R. Doubleday, P.C. Unangst, B.D. Roth, V.G. Beylin, R.B. Gilbersten, K. Chan, D.J. Schrier, A. Guglietta, D.A. Bornemeier, R.D. Dyer, J. Med. Chem. 42 (1999) 1161–1169.
[12] C.B. Chapleo, M. Myers, P.L. Myers, J.F. Saville, A.C.B. Smith, M.R. Stillings, I.F. Terlloch, D.S. Walter, A.P. Welbourn, J. Med. Chem. 42 (1986) 2273–2280.
[13] C.B. Chapleo, P.L. Myers, A.C. Smith, M.R. Stillings, I.F. Tulloch, D.S. Walter, J. Med. Chem. 31 (1988) 7–11.
[14] S. Turner, M. Myers, B. Gadie, A.J. Nelson, R. Pape, J.F. Saville, J.C. Doxey, T.L. Berridge, J. Med. Chem. 31 (1988) 902–906.
[15] S. Turner, M. Myers, B. Gadie, S.A. Hale, A. Horsley, A.J. Nelson, R. Pape, J.F. Saville, J.C. Doxey, T.L. Berridge, J. Med. Chem. 31 (1988) 907–915.
[16] J.Y. Chou, S.Y. Lai, S.L. Pan, G.M. Jow, J.W. Chern, J.H. Guh, Biochem. Pharmacol. 66 (2003) 115–124.
[17] P.M. Ronad, M.N. Noolvi, Eur. J. Med. Chem. 45 (2010) 85–89.
[18] S.N. Manjula, M.N. Noolvi, Eur. J. Med. Chem. 44 (2009) 2923–2929.
[19] A.K. Gadad, M.B. Palkar, M.N. Noolvi, B.S. Tippeswamy, Bioorg. Med. Chem. 16 (2008) 276–283.
[20] K.M. Honorio, R.C. Garratt, I. Polikarpova, A.D. Andricopulo, J. Mol. Graph. Model. 2 (2007) 921–927.
[21] K.M. Honorio, R.C. Garratt, I. Polikarpova, A.D. Andricopulo, Bioorg. Med. Chem. Lett. 15 (2005) 3119–3125.
[22] G. Tu, S. Li, H. Huang, G. Li, F. Xiong, X. Mai, H. Zhu, B. Kuang, W.F. Xu, Bioorg. Med. Chem. 16 (2008) 6663–6668.
[23] G. Kolavi, V. Hegde, I.A. Kazi, P. Gadad, Bioorg. Med. Chem. 14 (2006) 3069–3080.
[24] D.J. Ecobichon, in: The Basis of Toxicology Testing, third ed., CRC Press, New York, 1997, pp. 43–86.
[25] H. Hurnafi, N. Bouanani, M. Aziz, H.S. Caid, N. Ghalim, S. Amrani, J. Ethnopharmacol. 109 (2007) 156–160.
[26] J.D. Bancroft, M. Gamble, in: Theory and Practice of Histological Techniques, fifth ed., Churchill Livingstone, Edinburgh, London, Melbourne, UK, 2008, pp. 53–121.
[27] A. Zlatkis, B. Zak, A.J. Boyle, J. Lab. Clin. Med. 41 (1953) 486–492.
[28] E. Vanhandel, D.B. Zilversmit, J. Lab. Clin. Invest. 50 (1957) 152–157.
[29] R.A. Venugopala, S. Ramakrishanan, Clin. Chem. 21 (1975) 1543–1552.
[30] H.U. Bergmeyer, E. Bernt, in: Methods of Enzymatic Analysis, vol. 2, Verlag Chemie/Academic, Weinheim/London, 1974, p. 735.
[31] S. Reitman, S. Frankel, Am. J. Clin. Pathol. 28 (1957) 56–63.
[32] P.R.N. Kind, E.J. King, J. Clin. Pathol. 7 (1954) 322–326.
[33] Website: http://www.rcsb.org/pdb/explore.do?structureId=1OSH.
[34] H. Zhong, L.M. Tran, L. Jenna, J. Mol. Graph. Mod. 28 (2009) 336–346.
[35] Third report of the National Cholesterol Education Program (NCEP) Expert Panel on detection, evaluation and treatment of high blood cholesterol in adults (adult treatment panel III) Final report, Circulation 106 (2002) 3143–3421.
[36] J.P. Malaspina, H. Bussiere, G.L. Clave, Atherosclerosis 40 (1981) 373–375.
[37] L. Shewchuk, A. Hassell, B. Wisely, W. Rocque, W. Holmes, J. Veal, L.F. Kuyper, J. Med. Chem. 43 (2000) 133–138.
[38] R.W. Edgar, T.T. Anne, B.M. Octerloney, Y. Derek, H. Anne, H.D. Scott, E. Byron, P. Christopher, T.H. Earnes, L. Karen, J.A. Krystal, W.R. David, M.G. Tona, S. Lisa, Cancer Res. 64 (2004) 6652–6659.
[39] H. Assefa, S. Kamath, K. John, J. Comput. Aided Mol. Des. 17 (2003) 475–493.